International Journal of Architectural, Civil and Construction Sciences
ISSN: 2415-1734
Vol:14, No:3, 2020

Comparing the Behaviour of the FRP and Steel Reinforced Shear Walls under Cyclic Seismic Loading in Aspect of the Energy Dissipation

H. Rahman, T. Donchev, D. Petkova

***Abstract*—**Earthquakes claim thousands of lives around the world annually due to inadequate design of lateral load resisting systems particularly shear walls. Additionally, corrosion of the steel reinforcement in concrete structures is one of the main challenges in construction industry. Fibre Reinforced Polymer (FRP) reinforcement can be used as an alternative to traditional steel reinforcement. FRP has several excellent mechanical properties than steel such as high resistance to corrosion, high tensile strength and light self-weight; additionally, it has electromagnetic neutrality advantageous to the structures where it is important such as hospitals, some laboratories and telecommunications. This paper is about results of experimental research and it is incorporating experimental testing of two medium-scale concrete shear wall samples; one reinforced with Basalt FRP (BFRP) bar and one reinforced with steel bars as a control sample. The samples are tested under quasi-static-cyclic loading following modified ATC-24 protocol standard seismic loading. The results of both samples are compared to allow a judgement about performance of BFRP reinforced against steel reinforced concrete shear walls. The results of the conducted researches show a promising momentum toward utilisation of the BFRP as an alternative to traditional steel reinforcement with the aim of improving durability with suitable energy dissipation in the reinforced concrete shear walls.

***Keywords*—**Shear walls, internal FRP reinforcement, cyclic loading, energy dissipation and seismic behaviour.

I. Introduction

THE problem of steel corrosion can be solved by alternative reinforcement of FRP bars which are more durable against corrosion, have lighter weight, reduced CO_2 emission during production and excellent mechanical properties. In addition, nonconductive properties of internal FRP reinforcement can be effective in usage for the hospitals and other structures containing sensitive laboratory equipment where electromagnetic neutrality is an important factor [1].

Previous studies have been made on the steel Reinforced Concrete (RC) shear walls by many researchers proving the effective use of steel reinforcement for them. However, construction of shear walls in multi-storey buildings in the earthquake prone regions reinforced with FRP bars calls for investigation of their behavior [2].

Mohamed et al. conducted studies on cyclic load behaviour of glass FRP (GFRP) RC shear wall. The study involved testing a shear wall totally reinforced with FRP bars. It was found that GFRP-reinforced shear wall can attain good strength and deformation capacity as well as reasonable energy dissipation [2].

Maleki et al. investigated application of GFRP for improving the seismic behavior of steel shear walls where medium scale specimens are tested under quasi-static loading. It was found that the GFRP laminates cause more uniform distribution of tension field within the infill plate [3].

Petkune et al. studied the performance of the steel shear walls subjected to previous seismic loading. The specimens are strengthened with GFRP wrapping to improve stiffness and energy dissipation and then subjected to quasi-static lateral loading. The results of the studies are conforming and the system show significant improvement in strength and energy dissipation capacities after GFRP wrapping [4].

II. Methodology

A. Design

The shear wall specimen represents a precast panel in moderate-rise building as depicted in Fig. 1. The height of all shear wall (h_w) was 1000 mm and the horizontal length (I_w) of the wall is also 1000 mm. The wall thickness (T_w) was 100 mm.

The size of the specimen wall was chosen to represent a 1:3 scale model of the full-scale shear wall. The sample was designed in such way that the internal part of the shear wall would represent a precast panel surrounded by the boundary elements at perimeter. The aspect ratio of the sample is 1 representing ratio of the wall height over width.

The walls were designed with 10 mm high yield steel bars as main reinforcement. Design of the BFRP reinforcement cage was a replica of the steel reinforcement design. All stirrups for both samples were 6 mm mild steel bars.

The wall was fixed in the bottom to a Parallel Flanged Channel (PFC) using 10 mm high yield steel bar anchors welded to the PFC. The PFC was welded to the Rectangular Hollow Section (RHS) to allow for the fixing bolts. The RSH was welded to a thick steel plate. The plate was designed to be bolted to the strong frame where testing was conducted. Bottom fixity can be seen in bottom connections diagram (Fig. 1).

B. Material

To construct the shear wall specimens a designed concrete mix was provided by an external supplier. The casting of the samples was executed during single day from one batch of concrete to ensure uniformity of the strength in samples.

Hamid Rahman is with the Kingston University London, United Kingdom (e-mail: htceinc@gmail.com).

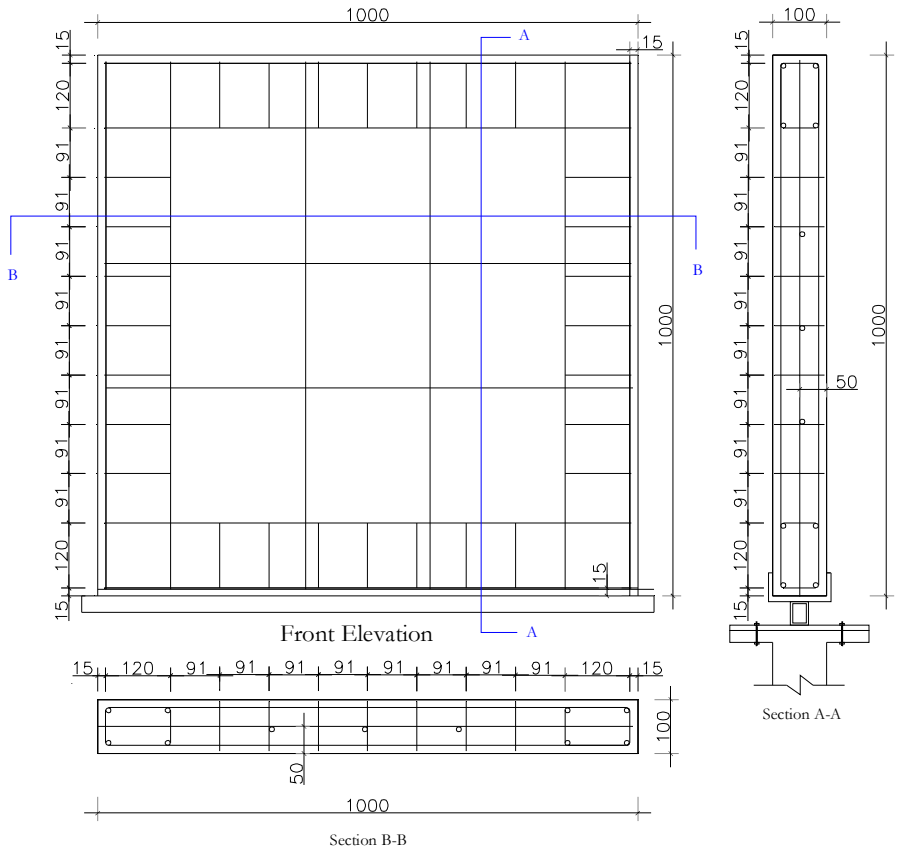

Fig. 1 Reinforcement cage

Combinations of the cylinders 150 x 300 mm and cubes 150 x 150 x 150 mm were casted to obtain uniaxial compressive strength of the concrete. The concrete strength was tested for each shear wall sample on the day of testing was estimated as C25/30.

The properties of the steel and BFRP [5] bars are indicated in Table I where d_b is the nominal diameter, A_b is the nominal cross-sectional area of bars, $E_{f/s}$ is the modulus of elasticity of FRP and steel and f_u is the ultimate tensile strength.

TABLE I
MECHANICAL PROPERTIES OF STEEL AND BFRP BARS

Specimen	Bar	d_b (mm)	A_b (mm^2)	$E_{f/s}$ (GPa)	F_u (MPa)
B10	BFRP	10	78.5	50	1000
S10	Steel	10	78.5	210	460

C. Instrumentation

Internal strain gauges by Micro Measurement VPG brand (Vishay) model CEA-06-240UZ-120 were applied using M-Bond 200 strain gauges adhesives and gauge bond surface cleanser and preparator by the same provider to measure the strains in all vertical bars and in a main horizontal bar [6].

Positions of the gauges were marked on the reinforcement cages; surface of the locations was smoothed by file and sand paper. All surfaces were well cleansed using isopropyl alcohol and M-Prep Conditioner 5. All surfaces were wiped free of chemical using M-Prep Neutralizer 5A by Vishay.

A combination of three gauges in two orthogonal directions and one diagonal direction (rosette gauges) was applied in the centre of the wall to measure in-plane strain in principal directions [7].

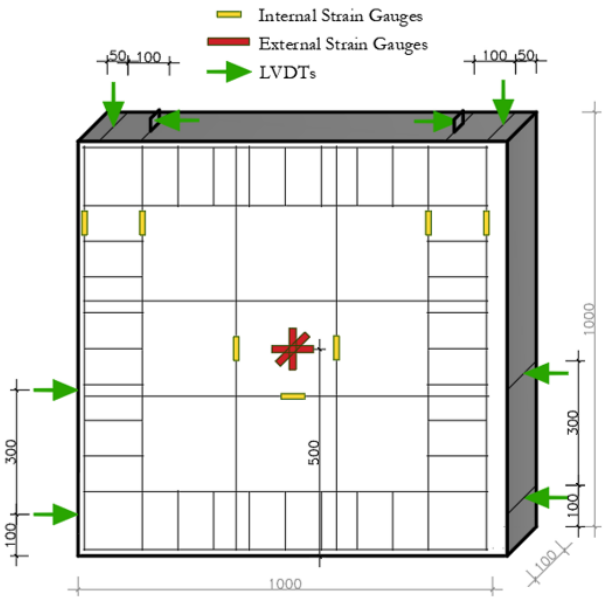

Fig. 2 Locations of the LVDTs, internal and external gauges

The LVDTs (Linear Variable Displacement Transducers) were attached between the strong frame and specimen. The LVDTs measured displacements of up to 50 mm. Fig. 2 shows the strain gauges and LVDTs.

D.Testing

The shear wall samples were installed and fixed in the bottom surface area to the strong reaction frame as illustrated in Fig. 3. The reaction frame was fully fixed in the strong concrete floor underneath. Screw jack was fully clamped to the strong reaction frame and metallic struts were installed below to prevent any deflection of the jack due to very heavy self-weight.

The lateral load is applied through jack model BD Benziler Screw Jack 500 kN to apply the quasi-static loading. The jack was fixed to the reaction frame by a rigid box made up of 35 mm thick square flat plates bolted with HSFG bolts 42 mm diameter.

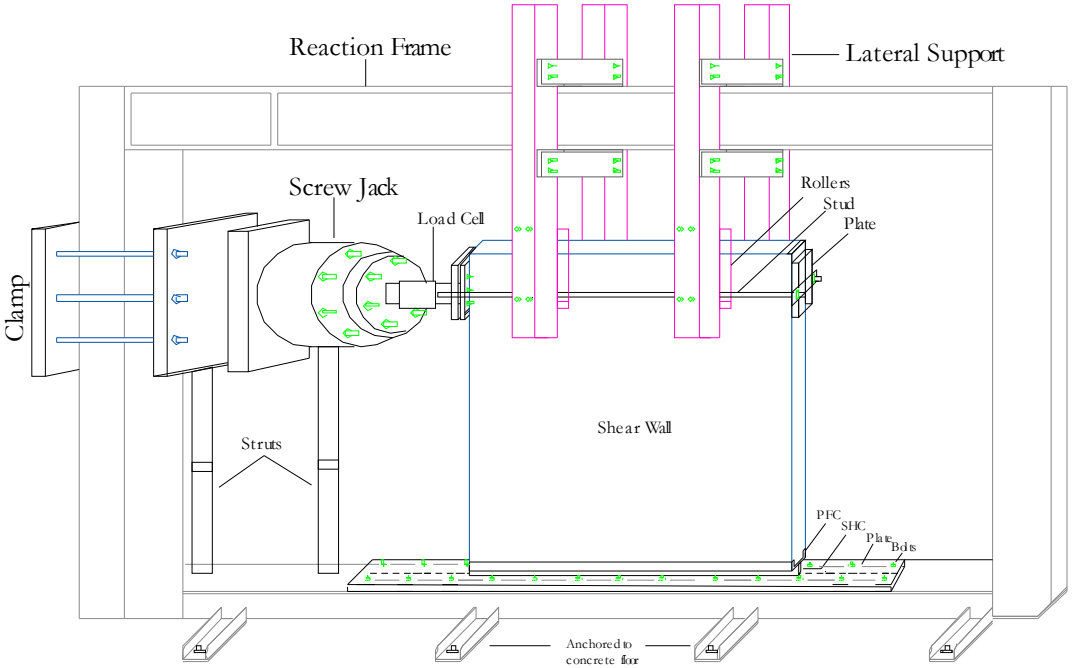

Fig. 3 Experimental test set up

The experimental programme comprised of testing RC shear wall samples under quasi-static cyclic loading until failure. The loads applied to make certain amount of displacement were recorded for each load cycle. One cycle of each load increment was used for each designated displacement. The load was controlled by using the designated software application and associated inverter to control the jack via signals send from the inverter to the motor.

The load waves were applied via the motor and the jack as smoothly as possible according to the recommendation of modified ATC 24 (1992) protocol [8]. Maximum of 12 cycles of load were applied to the test specimen and cracks were recorded against the cycles and its corresponding load magnitude. The loading was stopped when the shear wall could not sustain more loads and failed. The recommended displacement load history against the number of cycles used in this experiment is indicated in Fig. 4.

III. Experimental Results

Generally, all the shear wall samples started to respond to the increase of the load with developing of shear/flexural cracks as it can be seen in Figs. 5 (a)-(d). There was no sign of premature failure such as shear, sliding, or anchorage failure.

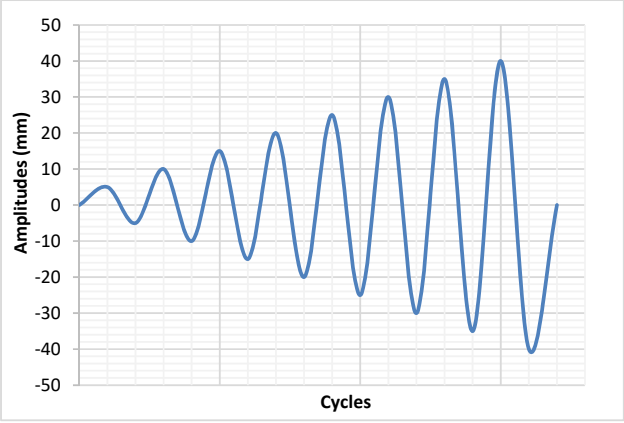

Fig. 4 Displacement history against cycles for quasi-static test per modified ATC-24 protocol

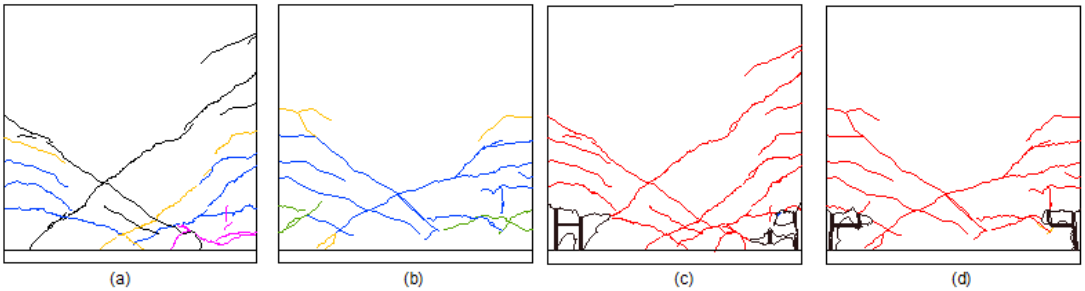

Fig. 5 Crack pattern; (a) S10, (b) B10. Crushing pattern, spalling and bar bending; (c) S10, (d) B10

TABLE II
BOTH SAMPLES' OBSERVATION SHEET

	0.2	0.4	0.8	1.2	2.5	3.5	5.0	10	15	20	25	30	35	40
S10	NOB	NOB	NOB	NOB	CKG	CKG	CKG	CSG/SPG	RKG	RKG	RKG	RKG	RKG	RKG
B10	NOB	NOB	NOB	CKG	CKG	CKG	BGN	CSG/SPG	SPG	RKG	RKG	BGN/SPG	RKG	RKG

NOB: No Observation, CKG: Cracking, BGN: Banging Noise, CSG: Crushing, SPG: Spalling, BRB: Bars Bending, RKG: Rocking.

Each of the samples exhibited a fairly symmetric lateral-load influenced cracking under pushing and pulling cyclic load conditions until there was a failure at one end of the wall as it can be seen in Fig. 5.

A. Crack and Crushing Patterns

The cracks started to appear and were developed as by green lines at 1.2 mm displacement, blue lines at 2.5 mm, yellow line at 3.5 mm, black lines at 5 mm and violet lines at 10 mm as it can be seen in Figs. 5 (a) and (b).

As the lateral displacement-controlled load continued to increase crushing, spalling of concrete appeared at the boundaries under compression and tension as it can be seen in Figs. 5 (c) and (d). As the displacement amplitudes increased more spalling of concrete cover become more evident at the compression and tension zones.

The red lines show all the cracks that have incurred during the 0.8 mm to 10 mm displacement amplitude while the black polylines in the bottom right and left of the samples show the crushed areas of the concrete simultaneous to the spalling of the concrete (Figs. 5 (c) and (d)).

Cracking and crushing of the concrete can also be seen in Figs. 6 (a) and (b). A major crack has formed in each of the samples approximately 1/5 of the height of the samples. As the displacement load increased the crack gap increased too.

All observations made during testing of the samples are enlisted in Table II. The observation started at an amplitude of 2.5 mm for SA6 and at an amplitude of 1.2 mm for BA10, BA6 and GA6.

The cracking continued until an amplitude of 5.0 mm for S10 and B10 samples; however, banging noise was recorded at an amplitude of 5.0 mm for the BFRP samples.

Spalling of the concrete cover occurred at an amplitude of 10 mm for the both samples. It continued to 15 mm amplitude and again in 30 mm amplitude for the B10 samples. This means that the B10 sample was stiffer than the concrete samples resulting in more spalling.

Crushing of the samples occurred at 10 mm amplitude and after this amplitude rocking of the both samples started. The rocking effect was when the samples split in to two parts in shear cracking zone and were acting like a mechanism.

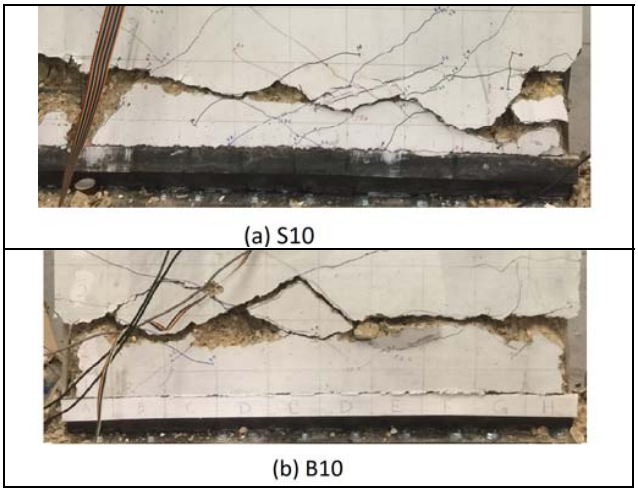

Fig. 6 Cracking and crushing photos for (a) S10, (b) B10 samples

B. Lateral Load – Top Displacement Hysteresis

The hysteresis graphs in Figs. 7 (a), (b) have a fair amount of symmetry under the pushing and pulling conditions. The figures show a wider loop for the B10 after a displacement amplitude of 3.5 mm; however, for S10 the loops are starting to widen at 10 mm amplitude due to intensive plastic deformation.

The loops continue to be wider for the S10 sample but it narrows after 20 mm displacement for the B10 sample. Both of the effects mean that S10 had higher energy dissipation due to good grip of concrete to the threaded bars.

Banging of the concrete occurred at 5 mm and 30 mm of amplitudes twice for the B10 samples which can mean that the concrete was broken due to higher flexibility of the BFRP reinforced sample than the concrete reinforced sample.

Crushing of the concrete occurred at 10 mm displacement amplitude hysteresis loop for the both S10 and B10 samples;

however, it was the first wide loop for the S10 sample and the second wide loop for the B10 sample which means that the BFRP reinforced sample was more flexibility before crushing due ductile nature of the BFRP reinforcements.

Rocking of the samples occurred at 15 mm and 20 mm of amplitude loops for S10 and B10 respectively as it can be seen in Figs. 7 (a) and (b). However, the loops in the S10 samples are much wider than the B10 sample due to the residual frictional forces of the threaded steel bars.

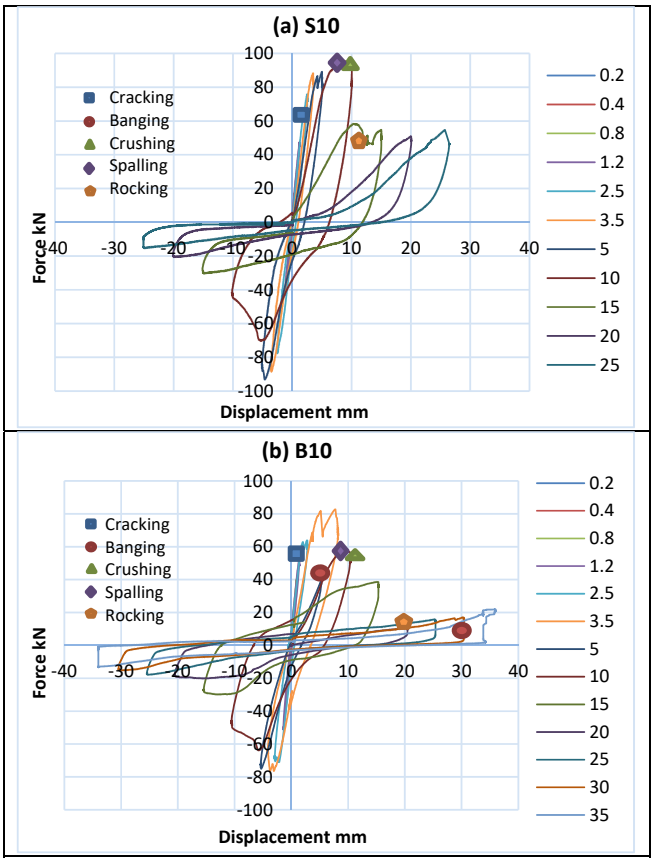

Fig. 7 Lateral force versus top-displacement relationship for S10 an B10 samples

C. Maximum and Minimum Points

The maximum and the minimum outlined points of the hysteresis response for all the samples are demonstrated in Fig. 8. Due to the destruction of the steel reinforced sample at 25 mm displacement the comparison between both shear walls since this point on is conducted only in this interval. The S10 response is shown in blue line and marker and the B10 sample behaviour is shown in grey line, marker and legends.

As in can be seen in the curves S10 sample with blue legends has a higher maximum and minimum response than the B10 sample in gray, this means that the steel reinforced sample was having a higher maximum and minimum response under the lateral cyclic loading.

Both the blue and the grey lines correspond more to each other under the negative period of loading than during the positive loading; therefore, calling for further analysis; hence, average of the maximum and minimum values need to be calculated.

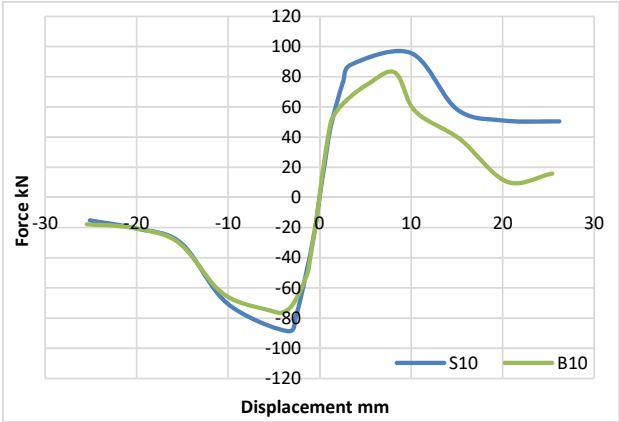

Fig. 8 Hysteresis maximum and minimum force against displacement graph for S10 and B10 sample

D. Average Maximum and Minimum Points

The average maximum and minimum points of the curve were taken from the previous analysis of the maximum and minimum value and the averaged values of the force against displacement values of each sample are depicted in Fig. 9.

The results show that S10 sample (blue line and markers) has a higher force against displacement response followed by the B10 sample (grey line and markers). Additionally, the S10 sample continues to sustain the load bearing capacity after 20 mm displacement amplitude which means that steel reinforced sample could resist higher loads but the BFRP also shows promising close results.

The initial response of the both samples is close to each other until a displacement amplitude of 2.5 mm after which the blue line takes about 10% to 20% higher forces per displacement amplitude. The BFRP sample could bear very close forces to the steel reinforced sample.

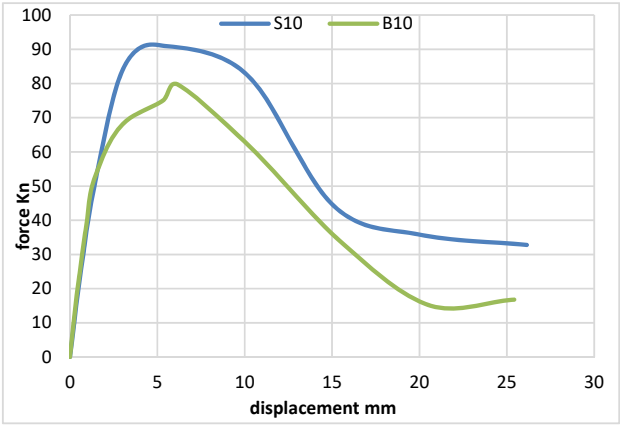

Fig. 9 Average maximum and minimum force-displacement graph for S10 and B10 samples

E. Cumulative Energy Dissipation

Cumulative Energy Dissipation (CED) in kNm against Displacement (mm) amplitude for all the samples is shown in Fig. 10. The curves in Fig. 10 have a similar behaviour until a CED of about 650 kNm at around 6 mm displacement amplitude. S10 rises to about 3200 kNm; B10 rises to about 2700 kNm at 20 mm displacement amplitude. S10 shows about 20% higher CED than B10 for the investigated interval of displacement.

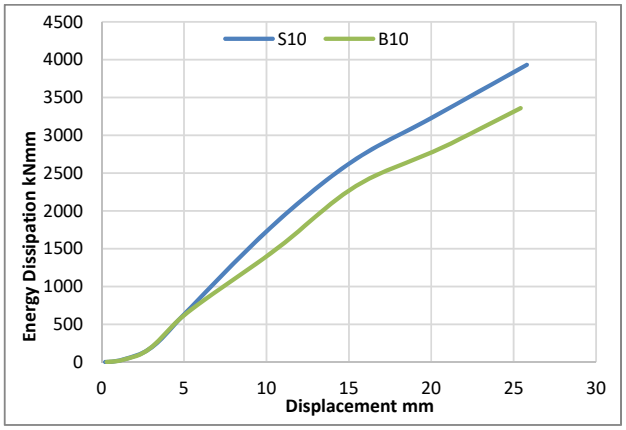

Fig. 10 Cumulative Energy Dissipation against displacement for the S10 and the B10 samples

IV. Conclusions

The experiments were conducted using the structural lab at Kingston University London and the following conclusions are drawn:

1. The ultimate capacity of BFRP reinforced shear wall sample is a bit less but close to the ultimate capacity of steel reinforced sample.
2. Steel reinforced sample shows a bit higher energy dissipation than the BFRP reinforced sample within the indicated interval of displacements.
3. The BFRP reinforced sample demonstrated better behaviour with further increase of the deformations and tendency for improving energy dissipation.

Generally, outcome of the researches shows a promising result for utilising BFRP as an alternative to traditional steel reinforcement for the concrete shear walls. Furthermore, for the future investigations we would recommend utilising anchorage for the reinforcement, applying higher strengths of concrete and investigating the behaviour of the walls in a wider interval of displacements.

References

[1] H. Rahman, T. Donchev, T. Petkova, D. Jurgelans and G. Hopartean, Behaviour of Concrete Shear Wall with BFRP Reinforcement for Concrete Structures, Proceedings of FRPRCS-14 Conference, Belfast, UK (2019)

[2] N. Mohamed, A. Farghaly, B. Benmokrane and K. Neale, Evaluation of GFRP-Reinforced Shear Walls, CSCE General Conference, Quebec Canada, May (2013)

[3] Maleki, A., Donchev, T., Hadavinia, H., Limbachiya, M. (2012) Improving the seismic resistance of structures using FRP/steel shear walls. Proc. 6th International Conference CICE 2012, Rome, Italy, 13-15 June 2012.

[4] Petkune, N., Donchev, T., Hadavinia, H., Limbachiya, M., Wertheim, D. (2016) Performance of pristine and retrofitted hybrid steel/fibre reinforced polymer composite shear walls. Construction and Building Materials, Elsevier, DOI 10.1016/j.conbuildmat.2016.05.013 ISSN 0950-0618

[5] MagmaTech, RockBar Brochure, link http://magmatech.co.uk/downloads/RockBar.pdf (2019)

[6] Micro Measurement A VPG Brand. General Purpose Strain Gauges – Linear Pattern; 2019. http://www.vishaypg.com/docs/11241/125uw.pdf

[7] Tokyo Measuring Instruments Lab, Concrete Material Use Strain Gauges; 2019. https://tml.jp/e/product/strain_gauge/concrete.html#p_list.html

[8] Applied Technology Council, 1992, "Guidelines for Cyclic Seismic Testing of Components of Steel Structures," ATC-24, Redwood City, CA.